Assessing species-specific neonicotinoid toxicity using cross-species chimeric nicotinic acetylcholine receptors in a *Drosophila* model

ANNA LASSOTA[1,2], JAMES J. L. HODGE[3] AND MATTHIAS SOLLER[1,2,4*]

[1]School of Biosciences, College of Life and Environmental Sciences, University of Birmingham, Edgbaston, Birmingham, B15 2TT, United Kingdom

[2]Birmingham Centre for Genome Biology, University of Birmingham, Edgbaston, Birmingham, B15 2TT, United Kingdom

[3]School of Physiology, Pharmacology and Neuroscience, University of Bristol, Biomedical Sciences building, University Walk, Bristol, BS8 1TD, United Kingdom

[4]Division of Molecular and Cellular Function, School of Biological Sciences, University of Manchester, Oxford Road, Manchester M13 9PT, United Kingdom

[*]Corresponding author: matthias.soller@manchester.ac.uk

Running title: Chimeric nAChRs for neonicotinoid toxicity in *Drosophila*

Key words: nAChR, neonicotinoids, *Apis mellifera*, *Drosophila*, CRISPR-Cas9 genome engineering, pesticides

Abstract

Nicotinic acetylcholine receptors (nAChRs) are ligand-gated ion channels and the main mediators of synaptic neurotransmission in the insect brain. In insects, nAChRs are pivotal for sensory processing, cognition and motor control, and are the primary target of neonicotinoid insecticides. Neonicotinoids are potent neurotoxins and pollinators such as honey bees are more sensitive and affected by extremely low sub-lethal doses. The pentameric nAChR channel is made up either of five α-subunits constituting five ligand-binding sites or a mixture of two to three α and β subunits constitute two to three ligand-binding sites. Of particular note, the honey bee nAChRα8 subunit is converted into a β subunit (nAChRβ2) in *Drosophila*, raising the question whether this α to β conversion makes flies less sensitive to neonicotinoids. To investigate species-specific aspects of neonicotinoid toxicity we CRISPR-Cas9 engineered a cross-species chimeric nAChR subunit by swapping the ligand-binding domain in *Drosophila* of nAChRβ2 with honey bee nAChRα8. Toxicity assessment by neonicotinoid thiamethoxam revealed significantly impaired motor functions in climbing and flight assays when comparing the α8/β2 chimeric channel to wild type or a β2 knock-out. However, both the α8/β2 chimeric channel and the β2 knock-out showed the same increased survival after neonicotinoid exposure compared to wild type flies. Combinatorial exposure to neonicotinoids also did not reveal differences. These findings highlight the critical role of nAChR subunit composition in motor control and demonstrate how subtle structural differences can profoundly impact motor function and pesticide response, offering new insights into the molecular mechanisms of neurotoxicity across species.

Introduction

Pesticides are indispensable for protecting global agricultural yields by reducing crop losses caused by pests [1]. Among these, neonicotinoids are highly effective due to their broad-spectrum efficacy and systemic activity, which enable integration into plant tissues for targeted pest control, and versatility in application methods, such as seed coating, to reduce environmental contamination [2,3]. Neonicotinoids exhibit high toxicity to insects, but not to vertebrates, making them safer alternatives to other classes of chemical [4,5]. However, neonicotinoids do not distinguish between pests and beneficial insects, and harm beneficial insects like honey bees, which are critical pollinators for both wild flora and agricultural crops [6–8]. The widespread decline of pollinators, partially attributed to pesticide exposure, poses significant ecological and economic challenges, highlighting the need for pest-control strategies with reduced non-target effects.

Honey bees, wild bees and other pollinators are adversely affected by extremely low sub-lethal doses of neonicotinoids (2 ng/ml compared to the LC50 dose of 4.28 µg/ml) impairing foraging behaviour, cognition, navigation and weakening of the immune system, and reducing reproductive success and genetic diversity within a colony [6,9–1415,1617–20]. Neonicotinoids, which target cholinergic neurotransmission, inhibit mushroom body Kenyon cell activity [21] and disrupt memory and olfactory sensory neuron activity in honey bees (*Apis mellifera*) and fruit flies (*Drosophila melanogaster*) [21–24].

The sensitivity of insects to neonicotinoids varies considerably between species, with honey bees being highly susceptible and *Drosophila* more resistant. For example, the 24-hour lethal concentration 50% (LC50) of thiamethoxam (TMX) is 3.13 µg/ml for adult *Drosophila* [25], whereas for honey bees it is 4.28 µg/ml [20]. This variation arises from differences in the repertoire of cytochrome P40 detoxification genes. *Drosophila* encodes 85 of these neonicotinoid-metabolising enzymes, whereas honey bees have only 46 [26,27]. Additionally,

honey bees have fewer antioxidant gene paralogs than *Drosophila*, which has an expanded antioxidant defence system. Since neonicotinoids can induce oxidative stress, this weaker antioxidant capacity may contribute to the greater sensitivity of bees compared to *Drosophila* [28].

Another reason contributing to this species-specific susceptibility could be the composition of nicotinic acetylcholine receptors (nAChRs). nAChRs are essential for neurotransmission, synaptic plasticity, and neuronal development, making prominent targets for neonicotinoid pesticides [29–32]. These pentameric cys-loop ligand-gated cation channels consist of α and β subunits forming homo- or heteropentamers. Ligand binding pockets, located at α-α or α-β interfaces, consist of loops A, B, and C from an α subunit and loops D, E, and F from the adjacent α or β subunit [33–35]. Importantly, β subunits lack the ability to form functional homopentamers due to the absence of loops A, B, and C [33,35]. Consequently, the subunit composition of nAChRs receptor affect their properties and determines susceptibility to agonists, such as acetylcholine or neonicotinoids (Fig. 1a).

Insects have relatively small nAChR gene families. *Drosophila melanogaster* encodes 10 subunits (Dα1-Dα7 and Dβ1-Dβ3), while the honey bee *Apis mellifera* encodes 11 (Amelα1-Amelα9 and Amelβ1-Amelβ2) [36]. α subunits are characterised by the presence of two adjacent cysteines in loop C of the ligand-binding domain (LBD), whereas β subunits lack these residues [35]. Notably, *Drosophila* encodes fewer α subunits compared to *Apis mellifera*. Instead, the *Drosophila* β2 subunit exhibits striking conservation with the honey bee Amelα8 subunit indicating a subunit conversion (Fig. 1b). However, the absence of loop C in *Drosophila* β2, which is essential for ion channel gating, highlights a structural divergence that may contribute to species-specific functional properties and differences in neonicotinoid susceptibility. Further, specific amino acid substitutions in nAChR subunits are known to impact insecticide susceptibility. For instance, *Drosophila* mutants lacking certain nAChR subunits or carrying

94 the natural variant R81T in the β1 subunit from aphids exhibit a 10- to 100-fold increase in
95 resistance to neonicotinoids [37–39].

96 Here, we examine the evolutionary divergence and functional implications of nAChR
97 subunits in *Drosophila melanogaster* and *Apis mellifera*. Phylogenetic analysis reveals that the
98 *Drosophila* β2 subunit has evolved from an ancestral α subunit. To investigate whether this
99 subunit conversion contributes to neonicotinoids sensitivity, we employed CRISPR-Cas9 gene-
100 editing technology to generate chimeric *Drosophila* flies expressing a chimeric nAChR
101 receptor. Specifically, we replaced the ligand-binding domain (LBD) of the *Drosophila* β2
102 subunit with that of the honey bee α8 subunit, providing a model to explore cross-species
103 receptor functionality. Behavioural and survival assays revealed significant impairments in
104 motor functions and altered sensitivity to insecticides, highlighting how structural differences
105 in receptor subunits can influence pesticide response. Our results provide insights into the
106 evolutionary trajectories of nAChR subunits and their roles in mediating neurotoxic compound
107 interactions, establishing a valuable *Drosophila* model for investigating cross-species pesticide
108 toxicity.

109

110 **Results**

111 **Species-specific specialization of *Drosophila* β2 subunit during evolution**

112 Insect *nAChRs* are classified into divergent subunits without clear orthologous
113 relationships between species, alongside a subset of genes that are highly conserved across taxa
114 [40]. Among these conserved subunits is the nAChRα8 subunit; however, it is absent in certain
115 Dipteran species, including *D. melanogaster*. Instead, the *Drosophila* β2 subunit exhibits
116 striking similarity to the honey bee α8 subunit, with 75% overall sequence identity and 92%
117 identity within the LBD indicating that α8 converted in to the β2 subunit (Fig. 1b and
118 Supplementary Fig. 1). Alphafold structural modelling further confirmed conservation of the

119 protein secondary structure of these two subunits, particularly in the LBD, with the exception
120 of the loop C (Fig. 1d) [41].

121 Next, to investigate whether *Drosophila* β2 represents a divergent lineage from other β
122 subunits or shares a closer evolutionary relationship with α subunits, we conducted a
123 phylogenetic analysis of all nAChR subunits in *D. melanogaster* and *A. mellifera*. Strikingly,
124 the analysis revealed that *Drosophila* β2 clusters within a clade predominantly composed of α
125 subunits, including α1–α4 and α8, indicating that *Drosophila* β2 is more closely related to α
126 subunits than to other β subunits (Fig. 1c). Interestingly, the honey bee β2 subunit exhibits
127 significant divergence and does not closely group with any other subunits, suggesting a
128 divergent evolutionary origin.

129

130 ***nAChR* subunits exhibit developmental dynamics and cell-specific distribution**

131 To investigate the expression patterns of *nAChR* subunits, we analysed tissue specific
132 expression data in adults, taking into account the enrichment values providing the gene
133 abundance measure in a tissue relative to that in the whole fly [42]. The majority of *nAChR*
134 subunits exhibits higher expression levels in females than in males (Fig. 2a). In both sexes,
135 *nAChR* subunits are predominantly expressed in the head, brain and CNS, and thoraco-
136 abdominal ganglion, with *Drosophila β2* being the most highly expressed subunit in the brain
137 and CNS. In other tissues, however, the levels of expression differ between sexes, with
138 *Drosophila β2* and *α7* being the most expressed subunits in the thoraco-abdominal ganglion of
139 males and females, respectively. Furthermore, only two subunits, *Drosophila α4* and *β3*, are
140 expressed across all tissues, with *Drosophila β3* showing notable expression in the heart.
141 Specific differences were observed between sexes. For instance, in the male salivary glands,
142 carcass, and crop, only *Drosophila α1*, *α2*, and *α3* were expressed, while *α4*, *β1*, and *β3* were
143 restricted to females.

144 Further, we investigated whether the expression of *nAChR* subunit changes during
145 development. Larval tissue analysis revealed that *Drosophila α3* is not expressed in any tissue
146 (Supplementary Fig. 2a), suggesting it is dispensable during development. In contrast,
147 *Drosophila β3* was expressed in all larval tissues, with the garland cells showing the highest
148 expression. The larval brain and CNS were the only tissues expressing all *nAChR* subunits, with
149 *Drosophila β3* showing the highest levels. Overall, *nAChR* subunit expression is relatively low
150 in most tissues in both larvae and adults (Fig. 2a and Supplementary Fig. 2a).

151 To refine the spatial expression of *β2* in *Drosophila* cells in more detail, we analysed
152 expression in single cells [43]. In whole adult flies, *β2* was found to be expressed in various cell
153 types, including neurons, sensory neurons, glial cells, as well as male germline and reproductive
154 system, however, its expression is not ubiquitous (Fig. 2b). Notably, a prominent cluster of
155 neurons classified as adult fly head CNS cells strongly expressed *β2*, suggesting it may have a
156 significant role in neuronal circuits [23,44]. Since *β2* displayed the highest expression levels in the
157 brain and CNS, we further analysed single cell expression data for the larval brain and whole
158 adult fly head. In adults, *β2* expression was observed in distinct neuronal populations,
159 contrasting with the broader expression of the neuronal marker *elav* (Fig. 2c-e) [45]. In contrast,
160 larval *β2* was colocalised with *elav* in the majority of CNS neurons (Supplementary Fig. 1b-d)
161 [46].

162 To validate the expression patterns, we used *nAChRβ2*$^{[2A\text{-}GAL4]}$ allele which has a *T2A-*
163 *GAL4* sequence fused at the 3' end of the gene, resulting in GAL4 expression as a separate
164 protein under the control of *nAChRβ2* regulation [47]. Therefore, we analysed both larval and
165 adult brains using nuclear *UAS-Histone2B-YFP* or membrane-tethered *UAS-mCD8-GFP*
166 reporters, co-staining neurons with anti-*elav* antibody. Consistent with our observations from
167 the single cell expression analyses, *β2* expression was restricted to specific neuronal
168 populations, confirming its non-ubiquitous distribution (Fig. 2f-k and Supplementary Fig. 1e-

169 j). Furthermore, we noticed enhanced *β2* expression in Kenyon cells, particularly when a
170 membrane-bound GFP reporter was used (Fig. 2i-k) [44].

171 Together, these findings reveal that nAChR subunit expression is dynamically regulated
172 during development and exhibits sex- and cell-specific specialisation, highlighting the
173 functional diversity of these receptors in neural circuits and other tissues. Furthermore, the
174 observed developmental shift in β2 expression, from widespread larval CNS expression to more
175 specialised adult neuronal populations, reflects the transition from simpler larval neural circuits
176 to the more specialised and complex adult CNS.

177

178 **Chimeric *Amelα8/Dβ2* ligand-binding domain flies are viable with impaired motor**
179 **functions**

180 Since the two adjacent cysteines in the loop C are essential for ligand binding in
181 nAChRs, we hypothesised that this difference may influence neonicotinoid susceptibility,
182 making honey bees more vulnerable. Therefore, we generated chimeric *nAChRβ2/α8*
183 ($nAChR\beta2^{Am\alpha8LBD}$) flies, where the *β2* LBD coding region in *Drosophila* was swapped with the
184 *Amelα8* LBD coding sequence using CRISPR-Cas9 genome engineering (Fig. 3a and
185 Supplementary Fig. 3). Successful recombinant flies were marked with *white+* selection
186 marker, disrupting the LBD, therefore resulting in a null allele ($nAChR\beta2^{nullA}$). To restore the
187 open reading frame (ORF) to generate a fly stock expressing the chimeric *nAChRβ2/α8* subunit
188 ($nAChR\beta2^{Am\alpha8LBD}$), the selection marker was then excised by PiggyBac transposase. Flies were
189 validated by polymerase chain reaction (PCR), Sanger sequencing, and subsequently by whole
190 genome sequencing.

191 To normalise the genetic background, we used trans-heterozygotic flies for the
192 $nAChR\beta2^{attP}$ allele ($nAChR\beta2^{nullB}$) in which the coding region was replaced with an *attP* site,
193 *3xP3-RFP* and a *loxP* site (Deng et al., 2019), together with the $nAChR\beta2^{nullA}$ allele. The

194 chimeric *nAChRβ2*^{Amα8LBD} mutants, as well as *nAChRβ2*^{nullA} and *nAChRβ2*^{nullB} flies are fully
195 viable when crossed with a chromosomal deficiency (n = 453, 275, 421, respectively).
196 To assess motor abilities, we performed negative geotaxis assays (Fig. 3b) and evaluated
197 flight ability (Fig 3c). In negative geotaxis assays the climbing ability of LBD swap mutant
198 (*nAChRβ2*^{Amα8LBD}/*nAChRβ2*^{nullB}) was greatly reduced ($p = 7.5*10^{-7}$) (Fig. 3b) compared to wild
199 type (WT). We did not detect significant differences in the *β2* null mutant
200 (*nAChRβ2*^{nullA}/*nAChRβ2*^{nullB}) nor the heterozygous mutant controls.
201 In flying ability assays, we observed the same, namely the LBD swap mutant
202 (*nAChRβ2*^{Amα8LBD}/*nAChRβ2*^{nullB}) were impaired ($p = 0.0066$) (Fig. 3c) compared to control flies,
203 but not the *β2* null mutant (*nAChRβ2*^{nullA}/*nAChRβ2*^{nullB}) or heterozygote mutant controls.
204
205 **Chimeric *Amelα8/Dβ2* ligand-binding domain flies display resistance to insecticides**
206 To investigate the impact of substituting the *Drosophila* β2 LBD with the honey bee
207 Amelα8 LBD on neonicotinoid susceptibility, we selected two well-characterised
208 neonicotinoids, TMX and imidacloprid (IMI), both of which exhibit high toxicity to pollinators
209 [5,39]. These compounds differ slightly in chemical structure and receptor specificity, with TMX
210 being one of the most potent full agonists of *Drosophila* and honey bee α1, α2, β1 and β2
211 combinations when heterologously expressed in frog oocytes and assayed by patch-clamp. In
212 contrast, IMI shows a stronger affinity for *Drosophila* β2-containing receptors compared to
213 TMX [39,48]. Both compounds target multiple nAChR subunits, enhancing their versatility broad-
214 spectrum toxicity [39].
215 In addition, we tested flupyradifurone (FPF), a systemic butanolide compound that is
216 chemically distinct from neonicotinoids and represents a novel alternative to these compounds
217 in pest management [49]. While FPF is not primarily targeted at *Drosophila* β2 subunits [39], its
218 broad-spectrum activity and demonstrated toxicity to non-target pollinators, including bees [50,51],

219 make it an important candidate for assessing cross-resistance and potential off-target effects
220 resulting from altered nAChR subunit composition.

221 First, we conducted survival analysis testing a range of TMX concentrations on WT
222 flies (Supplementary Fig. 4a, b). Fly viability was measured over 6 days. Based on the survival
223 curves, three different TMX concentrations were used for the toxicity experiments.

224 At 10 μM TMX, wild type flies had 43.75% survival after 144 h, while
225 *nAChRβ2*$^{Am\alpha8LBD}$/+, *nAChRβ2*^{nullA}/+, *nAChRβ2*^{nullB}/+, *nAChRβ2*^{nullA}/*nAChRβ2*^{nullB}, and
226 *nAChRβ2*$^{Am\alpha8LBD}$/*nAChRβ2*^{nullB} flies remained viable (Fig. 4a). At 20 μM, survival rates
227 declined progressively across all genotypes, with *nAChRβ2*^{nullA}/*nAChRβ2*^{nullB} mutants showing
228 the highest survival rates, followed by *nAChRβ2*$^{Am\alpha8LBD}$/*nAChRβ2*^{nullB} flies retaining more than
229 90% viability on day 6. This contrasted with *nAChRβ2*^{nullA}/+ (71.25%), *nAChRβ2*^{nullB}/+ (60%),
230 *nAChRβ2*$^{Am\alpha8LBD}$/+ (35%), and WT (11.25%) (Fig. 4b). At 40 μM, similar trend was observed,
231 although the viability of all flies was decreased below 50%. *nAChRβ2*^{nullA}/*nAChRβ2*^{nullB}
232 mutants retained by 48.75% day 6, followed by *nAChRβ2*$^{Am\alpha8LBD}$/*nAChRβ2*^{nullB} (41.25%),
233 *nAChRβ2*^{nullA}/+ (35%), *nAChRβ2*^{nullB}/+ (16.25%), *nAChRβ2*$^{Am\alpha8LBD}$/+ (3.33%), while WT flies
234 showed 0% survival by day 4 (Fig. 4c). Interestingly, apart from the trans-heterozygous
235 β^{nullA}/β^{nullB} flies, all genotypes experienced a sharp drop in viability between the 1st and 2nd day
236 of treatment, particularly *nAChRβ2*$^{Am\alpha8LBD}$/+ dropping from 62.5% to 30% and WT failing from
237 79% to 20%.

238 While both neonicotinoids and butenolides act as nAChR agonists, bind to the same site
239 and cause prolonged activation, they vary in the binding dynamics, receptor subtype
240 preferences, and potential to develop resistance [52]. To assess whether combining neonicotinoids
241 and butanolides results in additive or synergistic toxicity, we subjected flies to a mixture of
242 TMX (20 μM) with either FPF (20 μM) or IMI (20 μM). In nature, pollinators and insects are
243 frequently exposed to multiple insecticides rather than a single compound, making it crucial to

244 understand potential interactions and cross-resistance effects [53,54]. The TMX concentration was
245 chosen based on prior survival analyses, where double mutant flies retained > 90% viability
246 (Fig. 4b), while WT flies showed significant susceptibility. We tested chimeric
247 *nAChRβ2*^{Amα8LBD}/*nAChRβ2*^{nullB} flies and *nAChRβ2*^{nullA}/*nAChRβ2*^{nullB} mutants to determine
248 whether altered receptor composition influences responses to dual insecticide exposure. Flies
249 were treated for six days, and viability on day six was analysed as a log-fold change relative to
250 WT control and TMX-only treatment (Fig. 4d). Notably, exposure to TMX in combination with
251 either FPF or IMI resulted in a slight increase in survival rates. However, the combined
252 treatment did not significantly alter overall insecticide susceptibility. As expected,
253 *nAChRβ2*^{Amα8LBD}/*nAChRβ2*^{nullB} flies and *nAChRβ2*^{nullA}/*nAChRβ2*^{nullB} mutants flies exhibited
254 significantly higher resistance compared to WT across all conditions.

255 Taken together, our findings demonstrate that *nAChRβ2*^{nullA}/*nAChRβ2*^{nullB} null mutants
256 as well as the LBD swap mutants *nAChRβ2*^{Amα8LBD}/*nAChRβ2*^{nullB} flies exhibit higher survival
257 rates upon exposure to TMX, reinforcing the role of *Drosophila* β2 in neonicotinoid
258 susceptibility. Further, exposure to combined neonicotinoid and butanolide treatments did not
259 significantly alter overall lethality compared to TMX treatment on its own, indicating that sub-
260 lethal doses of these nAChR-targeting insecticides do not act synergistically in this context.
261 The observed resistance of chimeric and β2^{null} mutants further highlights the functional
262 divergence of Amelα8 in modifying nAChR-mediated insecticide susceptibility.

263

264 **Discussion**

265 The agricultural industry relies on pesticides to protect crops and maintain a stable food
266 supply for a growing population. Among these, neonicotinoids are the most widely used
267 insecticides due to their high efficacy and systemic action, reducing the need for repeated
268 applications. However, residues in nectar and pollen pose a significant risk to pollinators.

269 Despite their well-documented toxicity to bees and other beneficial insects, neonicotinoids
270 remain the dominant insecticides worldwide [55], highlighting the urgent need to mitigate their
271 ecological impact.

272 Beyond their effects on pollinators, neonicotinoids exhibit cross-species variability in
273 toxicity, with *Drosophila melanogaster* showing notably higher resistance than honey bees,
274 despite both species having homologous nAChRs [48]. The mechanisms underlying this
275 differential sensitivity remain unclear but are likely influenced by differences in receptor
276 composition, metabolism, or detoxification pathways [26,28]. To investigate species-specific
277 differences in neonicotinoid sensitivity, we established a *Drosophila* model where we swapped
278 the LBD of *D. melanogaster* β2 with honey bee Amelα8 subunit. The LBD swap mutant did
279 not reveal increased sensitivity to neonicotinoids compared to the *Drosophila* β2 null mutant.
280 However, the LBD swap mutant displayed motor function deficits indicating that this chimeric
281 receptor is functional. Minor structural changes in receptor subunits can profoundly impact
282 pharmacological properties [33,35,38,39] and could account for the altered neonicotinoid responses
283 observed in LBD chimeric mutant flies.

284 Previous studies in honey bees revealed tissue-specific expression of nAChR subunits,
285 including α2, α8 and β1 in Kenyon cells, while α7 was restricted to antennal lobe neurons [56]. A
286 similar functional diversity is observed in *Drosophila*, where nAChR subunits like α1 and α6
287 contribute to dendrite morphogenesis and synaptic transmission within larval visual circuits [57].
288 The absence of α3 expression in *Drosophila* larvae, combined with reduced nAChR subunit
289 expression during early developmental stages, suggests that receptor composition undergoes
290 developmental reprogramming to support the formation of complex adult neural circuits. This
291 dynamic tissue-, sex-, and stage-specific expression underscores the diverse roles of nAChRs,
292 including potential adaptations for behaviours such as reproduction [58,59]. Interestingly, in the
293 cockroach *Periplaneta americana*, subchronic exposure to sublethal doses of imidacloprid

294 induces a significant decrease in α2 mRNA expression, which correlates with a reduced
295 sensitivity to the insecticide [60], highlighting potential adaptive changes in nAChR subunit
296 composition even in fully developed insects.

297 Furthermore, high *Drosophila* β2 expression levels in CNS-specific neuronal
298 populations, including Kenyon cells, suggest its involvement in higher-order neuronal functions
299 such as learning and memory [44]. Similarly, honey bee α8 is enriched in honey bee mushroom
300 bodies [36,61,62], suggesting a conserved role for *Drosophila* β2 and honey bee α8 in regulating
301 mushroom body function across insect taxa, despite species-specific specialisations. Notably,
302 it has been shown that exposure to neonicotinoid insecticides affects cell activity in mushroom
303 body, and impairs learning and memory in insects, including *Drosophila* and honey bees [21–
304 23,63], further highlighting the critical role of nAChRs in cognitive functions and suggesting that
305 disruption of these receptors can have detrimental effects on neuronal processes related to
306 behaviour and learning.

307 Pharmacological and genetic studies have identified α1, α2, β1, and β2 as the primary
308 mediators of neonicotinoid toxicity [40,48,64]. Here, we generated a cross-species chimeric nAChR
309 using CRISPR-Cas9 genome engineering to evaluate neonicotinoid sensitivity in a *Drosophila*
310 model. Our study reveals that the *Drosophila* β2 conversion of honey bee α8 is not a main
311 determine of neonicotinoid sensitivity requiring to expand this approach to the other main
312 mediators of neonicotinoid toxicity. Our study establishes a framework for investigating
313 molecular determinants of neonicotinoid sensitivity of insects and vertebrates nAChR using a
314 cross-species chimeric nAChR *Drosophila* model. This model can contribute to the design of
315 next generation of insecticides for enhanced species-specific responses with implications for
316 pollinator conservation and pesticide safety for vertebrates including humans.

317

318 **Materials and methods**

319 **Fly stocks, genetics, immunostaining of tissues and imaging**

320 *D. melanogaster* CantonS and w^{1118} were used as the wild type control. *nAChRβ2*^{attP}
321 (BDSC 84545) and *nAChRβ2*$^{[2A\text{-}GAL4]}$ (BDSC 84666) stocks were described previously [47] and
322 were together with the chromosomal deficiency (BDSC 24996) from Bloomington. Fly crosses
323 were maintained at 25°C in plastic vials containing 10 ml of a standard cornmeal/yeast-rich
324 medium (1% agar, 2% yeast, 7% dextrose, 8% cornmeal w/v and 2% Nipagin from a 10%
325 solution in ethanol) with a 12:12 h light–dark cycle.

326 Third instar wandering larvae and adult brains from the progeny of *UAS-Histone2B-*
327 *YFP/+;nAChRβ2*$^{[2A\text{-}GAL4]}$*/+* and *UAS-mCD8-GFP/+;nAChRβ2*$^{[2A\text{-}GAL4]}$*/+* were dissected in
328 phosphate buffered saline (PBS) and fixed in 4% paraformaldehyde in PBT (PBS with 0.1%
329 TritonTM X-100 (Sigma-Aldrich, T8787)) for 30 min, followed by washes in PBT 3 × 15 min.
330 Samples were incubated overnight at 4°C with primary mouse anti-*elav* antibodies (MAb 7D,
331 1:20) [65], followed by secondary antibodies conjugated with Alexa Fluor 546 again overnight at
332 4°C. Samples were counterstained with DAPI (1:1000), mounted in Vectashield (Vector Labs),
333 scanned with Leica SP8, and processed using FIJI.

334

335 **Sequence analysis and single cell expression data visualisation**

336 Amino acid sequences were aligned using ClustalW with Megalin (DNAstar) or with
337 MAFFT [66] and phylogenetic trees were generated in NGPhylogeny.fr [67–69] and visualised using
338 iTOL [70].

339 Raw whole-genome sequencing reads were assessed for quality using FastQC, followed
340 by adapter trimming and quality filtering with Trim Galore. High-quality reads were aligned to
341 the *Drosophila melanogaster* (dm6) and *Apis mellifera* (Amel_HAv3.1) reference genomes
342 using BBMap. Mapping quality and coverage were evaluated, and alignments were visualized
343 using IGV (Integrative Genomics Viewer).

344 Single cell expression data was visualised as t-distributed stochastic neighbour
345 embedding (tSNE) from the 10x Stringent dataset in Scope and ASAP [71].
346
347 **Generation of chimeric *nAChRα8β2* flies**
348 Two single guide RNAs (sgRNAs) flanking the ligand binding domain *Dβ2* were
349 designed using PlatinumCRISPr [72] (Supplementary Fig. 3a, b) and cloned into *pUC-3GLA*
350 using the following primers: nACHr8 sgRNA left F1
351 (AAGATATCCGGGTGAACTTCGCTTATTGGAGCTAGGAAAGGTTTTAGAGCTAGA
352 AATAGC) and nACHr8 sgRNA right R1
353 (GCTATTTCTAGCTCTAAAACCACATGGCACAATCAAATTCGACGTTAAATTGAAA
354 ATAGG) as described [72]. Chimeric nAChR subunits were constructed by combining sequences
355 of *nAChRα8* from *A. mellifera* and *nAChRβ2* from *D. melanogaster* in three steps
356 (Supplementary Fig. 3c-e). Fragments used for generating the chimeric nAChR subunit were
357 synthesised using PCR with primers Bee alpha8 F2
358 (GGGAGTGGTCATTGCCATCTCAACCCTATATAAATTTG) and Bee alpha8 R2
359 (GGAATGTAATACCCACGCAAGGAATTATTAAG), followed by Bee alpha8 F1
360 (GCCAGTGAATTCGAGCTCGGTACCGCAGCTAGCGAAGCAAATCCTGACACAAAG
361 AGACTTTATGATGAC) and Bee alpha8 R1
362 (TTTACGCAGACTATCTTTCTAGGGTTAACCGTATAGAATAATGTTTTTCTTCGCAT
363 TG) for Amelα8 ligand binding domain, Dmel nAChRb left F1
364 (CGGCCAGTGAATTCGAGCTCGGTACCGATCCTTTTAGATAAAACATTTAGGAGCT
365 ATC) and nAChRsgmut left R1
366 (CTCTTTGTGTCAGGATTTGCTTCGAAACTCACTGGAGCCGTGAGAGGAGGGGTA
367 ATTCAGGGGAAAAACAGAGAAAAATGCC) for Dβ2 left homology arm, and
368 nAChRsgmut right F1

369 (ATTTTACGCATGATTATCTTTAACGTACGTCACAATATGATTATCTTTCTAGGGTT
370 AATCTGATTGTGCCCTGCGTAGCTTTAACATTCC) and Dmel alpha8 right R1
371 (GCATGCCTGCAGGTCGACTCTAGAGGATCCTGATAGTTGCTGCTGCGAATGCGG
372 AGCTG) for Dβ2 right homology arm, ensuring sgRNA sites in both homology arms are
373 mutated. Mutations were introduced based on conservation of the region between closely
374 related *Drosophila* species analysed using the UCSC genome browser
375 (https://genome.ucsc.edu) as described [73]. Fragments were then cloned stepwise into the *pUC19*
376 *pBac w+* containing *white* + marker, disrupting the LBD, therefore resulting in *nAChRβ2*^{null}
377 flies. The selection marker was flanked with inverted terminal repeats inserted at a TTAA
378 PiggyBac motifs for the later scarless excision by PiggyBac transposase.

379 The *pUC19 pBac w+ Amelα8/Dβ2* plasmid was treated with the nicking endonuclease
380 *Nb.Bts*I (NEB, R0707S) prior injection. Transgenic lines were generated by injection into a
381 GFP nosCas9 carrying flies (kindly provided by FlyORF). Positive transformants were
382 identified by red eye colour.

383 For *Drosophila* whole genome sequencing, large fragment DNA was extracted with the
384 Quick-DNA Tissue/Insect Miniprep Kit (Zymogene) according to the manufacturers'
385 instructions but replacing the BashingBead lysis step with cracking flies in liquid nitrogen
386 followed by gentle homogenization with a pestle in the provided BashingBead Buffer. Illumina
387 sequencing was done by Novogene and the sequence submitted to GEO [PRJNA1233772].

388

389 **Locomotive assessment**

390 Negative geotaxis experiments were done as previously described [74]. Briefly, two to five
391 day-old flies of both sexes were collected with CO_2 anaesthesia and grouped in sets of 20. Flies
392 were allowed to recover for a day and then placed in two inverted fly vials (19 cm). Flies were
393 tapped to the bottom, and their climbing behaviour was recorded on video. Every 5 s for a total

394 of 30 s, the distance climbed by each fly was measured and recorded. The data was collected
395 for four biological replicates.
396 For flying ability assessment, two to five day-old flies of both sexes were collected with
397 CO_2 anaesthesia and grouped in sets of 10. Flies were allowed to recover for a day before the
398 flying test. Then, flies were tapped to a flat surface, and their ability to fly was recorded on
399 video. Flies were observed over a 30 s period. At the end of 30 s, the number of flies that
400 successfully flew away was recorded. The data was collected for four biological replicates.
401
402 **Insecticide toxicity assay**
403 Two to five day-old flies of both sexes, grouped in sets of 20, were exposed to various
404 concentrations of thiamethoxam (Sigma-Aldrich, 37924), or a combination of 20 μM of
405 thiamethoxam with 20 μM imidacloprid (Thermo Fisher, 466752500) or 20 μM flupyradifurone
406 (MCE, HY-145295). The insecticides were dissolved in 0.01% acetone and added on top of the
407 standard fly food, and flies were added to the vials after 24 h. Exposure concentrations ranged
408 from 1.25 μM to 80 μM for survival curve analysis (Supplementary Fig. 4) and from 5 μM to
409 40 μM for testing all genotypes. Flies were exposed for 6 days, and survival was assessed every
410 24 h.
411
412 **Statistical analysis**
413 Statistical analyses were carried out using GraphPad Prism 9, applying one-way
414 ANOVA for behavioural assays or two-way ANOVA for the toxicity assays followed by
415 Tukey's test for pairwise comparisons. The data represent a minimum of three independent
416 replicates conducted on separate days.
417
418 **Acknowledgments**

We thank the Bloomington stock centre and FlyORF for fly lines, FlyORF for *Drosophila* injection service for embryo injections, and Al Handler for the PiggyBac plasmid

Authors' contributions

A.L. performed all experiments and analysed data. M.S. and J.J.L.H. conceptualised the project. A.L. wrote the manuscript and M.S. and J.J.L.H. reviewed it. All authors read and approved the final manuscript.

Funding

This work was supported by the Biotechnology and Biological Sciences Research Council to M.S. and J.J.L.H.

Availability of data and materials

The data generated or analysed during this study are included in the supplementary information in the supplementary information files. Whole genome sequencing data have been deposited at GEO under the accession number PRJNA1233772. The sequence for the *pUC19 pBac w+* has been deposited in GenBank and the plasmid is available from Addgene and the European plasmid repository.

Declarations:

Ethics approval and consent to participate

Not applicable.

Consent for publication

Not applicable.

444

445 **Competing interests**

446 The authors declare no competing interests.

447

448 **Figure Legends**

449 **Figure 1: Highly conserved *Drosophila* β2 subunit originated from an alpha subunit in**

450 **other insects**

451 (a) Schematic representation of homo- and heteropentameric nAChR receptors in insects

452 exhibiting different compositions of α (blue) and β (pink) subunits, with their active ligand

453 binding sites represented by ligands (cyan).

454 (b) Amino acid alignment of *D. melanogaster* β2 and honey bee Amelα8 subunits. Identical

455 amino acids are marked as red, complementary amino acid substitutions are labelled orange,

456 and non-complementary amino acid substitutions remained unmarked. The ligand binding

457 domain is underlined.

458 (c) Molecular phylogenetic analysis of all nAChR subunits present in *Drosophila* and honey

459 bee with two major α subunits clades highlighted with light blue and pink (subunits highly

460 conserved with mammalian α7). Species codes are Dm: *D. melanogaster* Amel: *A. mellifera*.

461 (d) Structural alignment of *D. melanogaster* β2 (blue) and honey bee α8 (pink) with all amino

462 acid differences in *D. melanogaster* ligand binding domain indicated (cyan).

463

464 **Figure 2: *Drosophila β2* is highly expressed in adult *Drosophila* brain and CNS but not in**

465 **every cell**

466 (a) Expression levels of *nAChR* subunits in female and male adult fly tissues.

467 (b) Visualisation of single cell expression for the *nAChRβ2* gene indicated in red with

468 annotation of the major cell clusters exhibiting *Dβ2* expression.

469 (c-e) Visualisation of single cell expression for *nAChRβ2* (c) and neuronal marker *elav* (d) or
470 both (e).

471 (f-k) Expression of *Dβ2* (f, i), *elav* (g, j) and merged (h, k) in adult *Drosophila* brains with
472 nuclear (f, h) and membrane-bound (i, k) *UAS* reporters. Scale bars are 20 µm.

473

474 **Figure 3: Chimeric *nAChRα8β2* flies exhibit locomotor defects**

475 (a) Schematic *Dβ2* gene model with the ligand binding domain swap indicated with coding
476 exons marked in pink. The *white+* selection marker was incorporated into the *nAChRβ2* gene
477 along with the honey bee *nAChRα8* LBD encoding fragment, generating a $nAChR\beta2^{null}$ allele.
478 The reading frame can be restored by excising the PiggyBac transposon.

479 (b) Climbing activity was assessed by negative geotaxis and is shown as means with the
480 standard error from four biologically independent groups (n=20). Statistically significant
481 differences are indicated by asterisks (****$p \leq 0.0001$).

482 (c) Flies of the indicated genotypes were tested for their flight ability shown as means with the
483 standard error from four biologically independent groups (n=10). Statistically significant
484 differences are indicated by asterisks (**$p \leq 0.01$).

485

486 **Figure 4: The α8 ligand binding domain does not sensitize flies to neonicotinoids**

487 (a-c) Flies viability exposed to 10 µM (a), 20 µM (b) and 40 µM (c) thiamethoxam measured
488 every 24 h for 6 days is shown as mean with standard error from four biologically independent
489 groups (n = 20).

490 (d) Survival rate of $nAChR\beta2^{Am\alpha8LBD}/nAChR\beta2^{nullA}$ and $nAChR\beta2^{nullA}/nAChR\beta2^{nullB}$ mutants
491 compared to WT flies subjected to different insecticides combinations. The log2 fold-change
492 shown as mean with standard error from four biologically independent groups (n = 20)
493 represents the viability of flies after six days of treatment with thiamethoxam (TMX) or TMX

494 mixed with imidacloprid (IMI) or flupyradifurone (FPF) in equimolar ratios. Statistically
495 significant differences are indicated with letters (a = *$p \leq 0.5$, b = **$p \leq 0.01$, c = ***$p \leq 0.001$,
496 d = ****$p \leq 0.0001$).
497

498 **References**

499 1. Fenik, J., Tankiewicz, M. & Biziuk, M. Properties and determination of pesticides in fruits and
500 vegetables. *TrAC Trends Anal. Chem.* **30**, 814–826 (2011).
501 2. Elbert, D. L., Mawuenyega, K. G., Scott, E. A., Wildsmith, K. R. & Bateman, R. J. Stable Isotope
502 Labeling Tandem Mass Spectrometry (SILT): Integration with Peptide Identification and Extension
503 to Data-Dependent Scans. *J. Proteome Res.* **7**, 4546–4556 (2008).
504 3. Jeschke, P., Nauen, R., Schindler, M. & Elbert, A. Overview of the Status and Global Strategy for
505 Neonicotinoids. *J. Agric. Food Chem.* **59**, 2897–2908 (2011).
506 4. Gibbons, D., Morrissey, C. & Mineau, P. A review of the direct and indirect effects of
507 neonicotinoids and fipronil on vertebrate wildlife. *Environ. Sci. Pollut. Res.* **22**, 103–118 (2015).
508 5. Casida, J. E. Neonicotinoids and Other Insect Nicotinic Receptor Competitive Modulators: Progress
509 and Prospects. *Annu. Rev. Entomol.* **63**, 125–144 (2018).
510 6. Henry, M. *et al.* A Common Pesticide Decreases Foraging Success and Survival in Honey Bees.
511 *Science* **336**, 348–350 (2012).
512 7. Pisa, L. W. *et al.* Effects of neonicotinoids and fipronil on non-target invertebrates. *Environ. Sci.*
513 *Pollut. Res.* **22**, 68–102 (2015).
514 8. Woodcock, B. A. *et al.* Impacts of neonicotinoid use on long-term population changes in wild bees
515 in England. *Nat. Commun.* **7**, 12459 (2016).
516 9. Crall, J. D. *et al.* Neonicotinoid exposure disrupts bumblebee nest behavior, social networks, and
517 thermoregulation. *Science* **362**, 683–686 (2018).
518 10. Gill, R. J., Ramos-Rodriguez, O. & Raine, N. E. Combined pesticide exposure severely affects
519 individual- and colony-level traits in bees. *Nature* **491**, 105–108 (2012).
520 11. Muth, F. & Leonard, A. S. A neonicotinoid pesticide impairs foraging, but not learning, in free-
521 flying bumblebees. *Sci. Rep.* **9**, 4764 (2019).
522 12. Rundlöf, M. *et al.* Seed coating with a neonicotinoid insecticide negatively affects wild bees. *Nature*
523 **521**, 77–80 (2015).

13. Tasman, K., Rands, S. A. & Hodge, J. J. L. Using radio frequency identification and locomotor activity monitoring to assess sleep, locomotor, and foraging rhythmicity in bumblebees. *STAR Protoc.* **2**, 100598 (2021).
14. Tasman, K., Rands, S. A. & Hodge, J. J. L. The Neonicotinoid Insecticide Imidacloprid Disrupts Bumblebee Foraging Rhythms and Sleep. *iScience* **23**, 101827 (2020).
15. Whitehorn, P. R., O'Connor, S., Wackers, F. L. & Goulson, D. Neonicotinoid Pesticide Reduces Bumble Bee Colony Growth and Queen Production. *Science* **336**, 351–352 (2012).
16. Forfert, N. *et al.* Neonicotinoid pesticides can reduce honeybee colony genetic diversity. *PLOS ONE* **12**, e0186109 (2017).
17. Annoscia, D. *et al.* Neonicotinoid Clothianidin reduces honey bee immune response and contributes to Varroa mite proliferation. *Nat. Commun.* **11**, 5887 (2020).
18. Decio, P. *et al.* Thiamethoxam exposure deregulates short ORF gene expression in the honey bee and compromises immune response to bacteria. *Sci. Rep.* **11**, 1489 (2021).
19. Di Prisco, G. *et al.* Neonicotinoid clothianidin adversely affects insect immunity and promotes replication of a viral pathogen in honey bees. *Proc. Natl. Acad. Sci.* **110**, 18466–18471 (2013).
20. Oliveira, R. A., Roat, T. C., Carvalho, S. M. & Malaspina, O. Side-effects of thiamethoxam on the brain andmidgut of the africanized honeybee *Apis mellifera* (Hymenopptera: Apidae). *Environ. Toxicol.* **29**, 1122–1133 (2014).
21. Palmer, M. J. *et al.* Cholinergic pesticides cause mushroom body neuronal inactivation in honeybees. *Nat. Commun.* **4**, 1634 (2013).
22. Smith, D. B. *et al.* Insecticide exposure during brood or early-adult development reduces brain growth and impairs adult learning in bumblebees. *Proc. R. Soc. B Biol. Sci.* **287**, 20192442 (2020).
23. Tasman, K., Hidalgo, S., Zhu, B., Rands, S. A. & Hodge, J. J. L. Neonicotinoids disrupt memory, circadian behaviour and sleep. *Sci. Rep.* **11**, 2061 (2021).
24. Tatarko, A. R., Leonard, A. S. & Mathew, D. A neonicotinoid pesticide alters Drosophila olfactory processing. *Sci. Rep.* **13**, 10606 (2023).
25. Li, X., Liu, J. & Wang, X. Exploring the multilevel hazards of thiamethoxam using Drosophila melanogaster. *J. Hazard. Mater.* **384**, 121419 (2020).

552 26. Berenbaum, M. R. & Johnson, R. M. Xenobiotic detoxification pathways in honey bees. *Curr. Opin.*
553 *Insect Sci.* **10**, 51–58 (2015).
554 27. Tasman, K., Rands, S. A. & Hodge, J. J. L. The Power of Drosophila melanogaster for Modeling
555 Neonicotinoid Effects on Pollinators and Identifying Novel Mechanisms. *Front. Physiol.* **12**,
556 659440 (2021).
557 28. Corona, M. & Robinson, G. E. Genes of the antioxidant system of the honey bee: annotation and
558 phylogeny. *Insect Mol. Biol.* **15**, 687–701 (2006).
559 29. Tomizawa, M. & Casida, J. E. Structure and diversity of insect nicotinic acetylcholine receptors.
560 *Pest Manag. Sci.* **57**, 914–922 (2001).
561 30. Role, L. W. & Berg, D. K. Nicotinic Receptors in the Development and Modulation of CNS
562 Synapses. *Neuron* **16**, 1077–1085 (1996).
563 31. Wessler, I. & Kirkpatrick, C. J. Acetylcholine beyond neurons: the non-neuronal cholinergic system
564 in humans. *Br. J. Pharmacol.* **154**, 1558–1571 (2008).
565 32. Tomizawa, M., Millar, N. S. & Casida, J. E. Pharmacological profiles of recombinant and native
566 insect nicotinic acetylcholine receptors. *Insect Biochem. Mol. Biol.* **35**, 1347–1355 (2005).
567 33. Matsuda, K. *et al.* Neonicotinoids: insecticides acting on insect nicotinic acetylcholine receptors.
568 *Trends Pharmacol. Sci.* **22**, 573–580 (2001).
569 34. Karlin, A. Emerging structure of the Nicotinic Acetylcholine receptors. *Nat. Rev. Neurosci.* **3**, 102–
570 114 (2002).
571 35. Ihara, M. *et al.* Crystal structures of Lymnaea stagnalis AChBP in complex with neonicotinoid
572 insecticides imidacloprid and clothianidin. *Invert. Neurosci.* **8**, 71–81 (2008).
573 36. Dupuis, J., Louis, T., Gauthier, M. & Raymond, V. Insights from honeybee (Apis mellifera) and fly
574 (Drosophila melanogaster) nicotinic acetylcholine receptors: From genes to behavioral functions.
575 *Neurosci. Biobehav. Rev.* **36**, 1553–1564 (2012).
576 37. Bass, C. *et al.* Mutation of a nicotinic acetylcholine receptor β subunit is associated with resistance
577 to neonicotinoid insecticides in the aphid Myzus persicae. *BMC Neurosci.* **12**, 51 (2011).

578 38. Homem, R. A. *et al.* Evolutionary trade-offs of insecticide resistance — The fitness costs associated
579 with target-site mutations in the nAChR of *Drosophila melanogaster*. *Mol. Ecol.* **29**, 2661–2675
580 (2020).
581 39. Lu, W. *et al.* Nicotinic acetylcholine receptor modulator insecticides act on diverse receptor
582 subtypes with distinct subunit compositions. *PLOS Genet.* **18**, e1009920 (2022).
583 40. Jones, A. K. & Sattelle, D. B. Diversity of Insect Nicotinic Acetylcholine Receptor Subunits. in
584 *Insect Nicotinic Acetylcholine Receptors* (ed. Thany, S. H.) vol. 683 25–43 (Springer New York,
585 New York, NY, 2010).
586 41. Jumper, J. *et al.* Highly accurate protein structure prediction with AlphaFold. *Nature* **596**, 583–589
587 (2021).
588 42. Krause, S. A., Overend, G., Dow, J. A. T. & Leader, D. P. FlyAtlas 2 in 2022: enhancements to the
589 *Drosophila melanogaster* expression atlas. *Nucleic Acids Res.* **50**, D1010–D1015 (2022).
590 43. Li, H. *et al.* Fly Cell Atlas: A single-nucleus transcriptomic atlas of the adult fruit fly. *Science* **375**,
591 eabk2432 (2022).
592 44. Barnstedt, O. *et al.* Memory-Relevant Mushroom Body Output Synapses Are Cholinergic. *Neuron*
593 **89**, 1237–1247 (2016).
594 45. Ustaoglu, P. *et al.* Dynamically expressed single ELAV/Hu orthologue elavl2 of bees is required
595 for learning and memory. *Commun. Biol.* **4**, 1234 (2021).
596 46. Brunet Avalos, C., Maier, G. L., Bruggmann, R. & Sprecher, S. G. Single cell transcriptome atlas
597 of the Drosophila larval brain. *eLife* **8**, e50354 (2019).
598 47. Deng, B. *et al.* Chemoconnectomics: Mapping Chemical Transmission in Drosophila. *Neuron* **101**,
599 876-893.e4 (2019).
600 48. Ihara, M. *et al.* Cofactor-enabled functional expression of fruit fly, honeybee, and bumblebee
601 nicotinic receptors reveals picomolar neonicotinoid actions. *Proc. Natl. Acad. Sci.* **117**, 16283–
602 16291 (2020).
603 49. Nauen, R. *et al.* Flupyradifurone: a brief profile of a new butenolide insecticide. *Pest Manag. Sci.*
604 **71**, 850–862 (2015).

605 50. Tosi, S. *et al.* Long-term field-realistic exposure to a next-generation pesticide, flupyradifurone,
606 impairs honey bee behaviour and survival. *Commun. Biol.* **4**, 805 (2021).
607 51. Siviter, H. *et al.* A novel pesticide has lethal consequences for an important pollinator. *Sci. Total*
608 *Environ.* **952**, 175935 (2024).
609 52. Crossthwaite, A. J. *et al.* The invertebrate pharmacology of insecticides acting at nicotinic
610 acetylcholine receptors. *J. Pestic. Sci.* **42**, 67–83 (2017).
611 53. Johnson, R. M., Dahlgren, L., Siegfried, B. D. & Ellis, M. D. Acaricide, Fungicide and Drug
612 Interactions in Honey Bees (Apis mellifera). *PLoS ONE* **8**, e54092 (2013).
613 54. Decio, P. *et al.* Acute thiamethoxam toxicity in honeybees is not enhanced by common fungicide
614 and herbicide and lacks stress-induced changes in mRNA splicing. *Sci. Rep.* **9**, 19196 (2019).
615 55. Sparks, T. C. *et al.* Insecticides, biologics and nematicides: Updates to IRAC's mode of action
616 classification - a tool for resistance management. *Pestic. Biochem. Physiol.* **167**, 104587 (2020).
617 56. Cens, T. *et al.* Molecular Targets of Neurotoxic Insecticides in *Apis mellifera*. *Eur. J. Org. Chem.*
618 **2022**, e202101531 (2022).
619 57. Rosenthal, J. S. *et al.* Temporal regulation of nicotinic acetylcholine receptor subunits supports
620 central cholinergic synapse development in *Drosophila*. *Proc. Natl. Acad. Sci.* **118**, e2004685118
621 (2021).
622 58. Komori, Y. *et al.* Functional impact of subunit composition and compensation on Drosophila
623 melanogaster nicotinic receptors–targets of neonicotinoids. *PLOS Genet.* **19**, e1010522 (2023).
624 59. Yoshinari, Y. *et al.* Neuronal octopamine signaling regulates mating-induced germline stem cell
625 increase in female Drosophila melanogaster. *eLife* **9**, e57101 (2020).
626 60. Bantz, A., Goven, D., Siegwart, M., Maugin, S. & Raymond, V. Exposure to a sublethal dose of
627 imidacloprid induces cellular and physiological changes in Periplaneta americana: Involvement of
628 α2 nicotinic acetylcholine subunit in imidacloprid sensitivity. *Pestic. Biochem. Physiol.* **181**,
629 105014 (2022).
630 61. Thany, S. H., Crozatier, M., Raymond-Delpech, V., Gauthier, M. & Lenaers, G. Apisα2, Apisα7-1
631 and Apisα7-2: three new neuronal nicotinic acetylcholine receptor α-subunits in the honeybee brain.
632 *Gene* **344**, 125–132 (2005).

633 62. Thany, S. H., Lenaers, G., Crozatier, M., Armengaud, C. & Gauthier, M. Identification and
634 localization of the nicotinic acetylcholine receptor alpha3 mRNA in the brain of the honeybee, *Apis*
635 *mellifera*. *Insect Mol. Biol.* **12**, 255–262 (2003).
636 63. Ferreira, L. C. *et al.* Disruption of exploratory behavior and olfactory memory in cockroaches
637 exposed to sublethal doses of the neonicotinoid Thiamethoxam. *Pestic. Biochem. Physiol.* **205**,
638 106167 (2024).
639 64. Perry, T. *et al.* Role of nicotinic acetylcholine receptor subunits in the mode of action of
640 neonicotinoid, sulfoximine and spinosyn insecticides in Drosophila melanogaster. *Insect Biochem.*
641 *Mol. Biol.* **131**, 103547 (2021).
642 65. Haussmann, I. U., Li, M. & Soller, M. ELAV-Mediated 3′-End Processing of *ewg* Transcripts Is
643 Evolutionarily Conserved Despite Sequence Degeneration of the ELAV-Binding Site. *Genetics*
644 **189**, 97–107 (2011).
645 66. Katoh, K. & Standley, D. M. MAFFT Multiple Sequence Alignment Software Version 7:
646 Improvements in Performance and Usability. *Mol. Biol. Evol.* **30**, 772–780 (2013).
647 67. Criscuolo, A. & Gribaldo, S. BMGE (Block Mapping and Gathering with Entropy): a new software
648 for selection of phylogenetic informative regions from multiple sequence alignments. *BMC Evol.*
649 *Biol.* **10**, 210 (2010).
650 68. Guindon, S. *et al.* New Algorithms and Methods to Estimate Maximum-Likelihood Phylogenies:
651 Assessing the Performance of PhyML 3.0. *Syst. Biol.* **59**, 307–321 (2010).
652 69. Lemoine, F. *et al.* NGPhylogeny.fr: new generation phylogenetic services for non-specialists.
653 *Nucleic Acids Res.* **47**, W260–W265 (2019).
654 70. Letunic, I. & Bork, P. Interactive Tree of Life (iTOL) v6: recent updates to the phylogenetic tree
655 display and annotation tool. *Nucleic Acids Res.* **52**, W78–W82 (2024).
656 71. David, F. P. A., Litovchenko, M., Deplancke, B. & Gardeux, V. ASAP 2020 update: an open,
657 scalable and interactive web-based portal for (single-cell) omics analyses. *Nucleic Acids Res.* **48**,
658 W403–W414 (2020).
659 72. Haussmann, I. U. *et al.* Structure-optimized sgRNA selection with PlatinumCRISPr for efficient
660 Cas9 generation of knockouts. *Genome Res.* **34**, 2279–2292 (2024).

661 73. McQuarrie, D. W. J. & Soller, M. Phylogenomic instructed target analysis reveals ELAV complex
662 binding to multiple optimally spaced U-rich motifs. *Nucleic Acids Res.* **52**, 12712–12726 (2024).
663 74. Haussmann, I. U. *et al.* CMTr cap-adjacent 2′-O-ribose mRNA methyltransferases are required for
664 reward learning and mRNA localization to synapses. *Nat. Commun.* **13**, 1209 (2022).
665

Figure 1

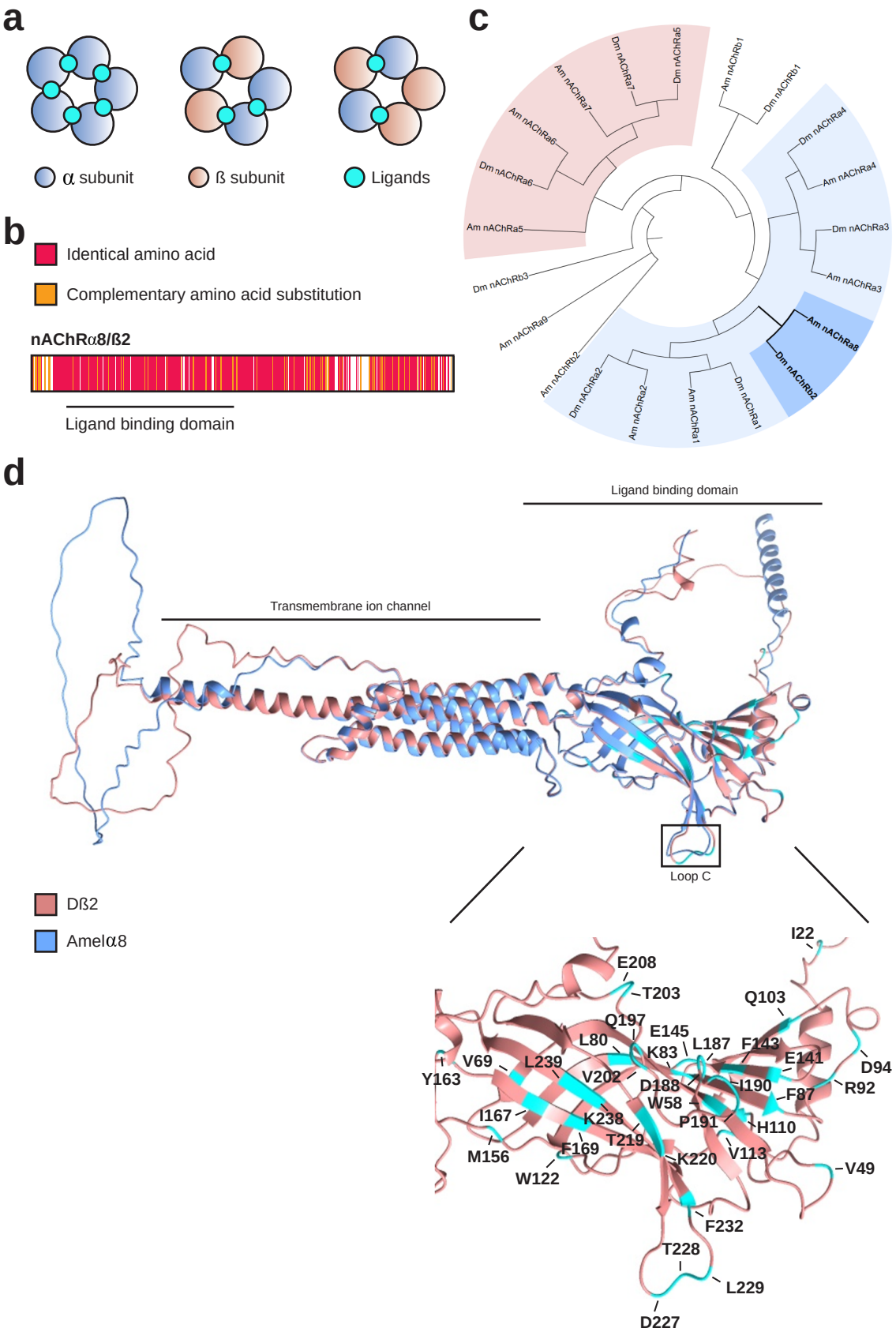
a
α subunit
ß subunit
Ligands
b
Identical amino acid
Complementary amino acid substitution
nAChRα8/ß2
Ligand binding domain
c
Dm nAChRa5
Dm nAChRa7
Am nAChRa7
Am nAChRa6
Dm nAChRa6
Am nAChRa5
Am nAChRb1
Dm nAChRb1
Dm nAChRa4
Am nAChRa4
Dm nAChRa3
Am nAChRa3
Dm nAChRb3
Am nAChRa9
Am nAChRb2
Dm nAChRa2
Am nAChRa2
Am nAChRa1
Dm nAChRa1
Am nAChRa8
Dm nAChRb2
d
Ligand binding domain
Transmembrane ion channel
Loop C
Dß2
AmelΔ8
I22
E208
T203
Q103
Q197
E145
L80
K83
L187
F143
E141
D94
V69
L239
Y163
V202
D188
I190
R92
F87
W58
I167
K238
P191
H110
T219
M156
F169
K220
V113
V49
W122
F232
T228
L229
D227

Figure 2

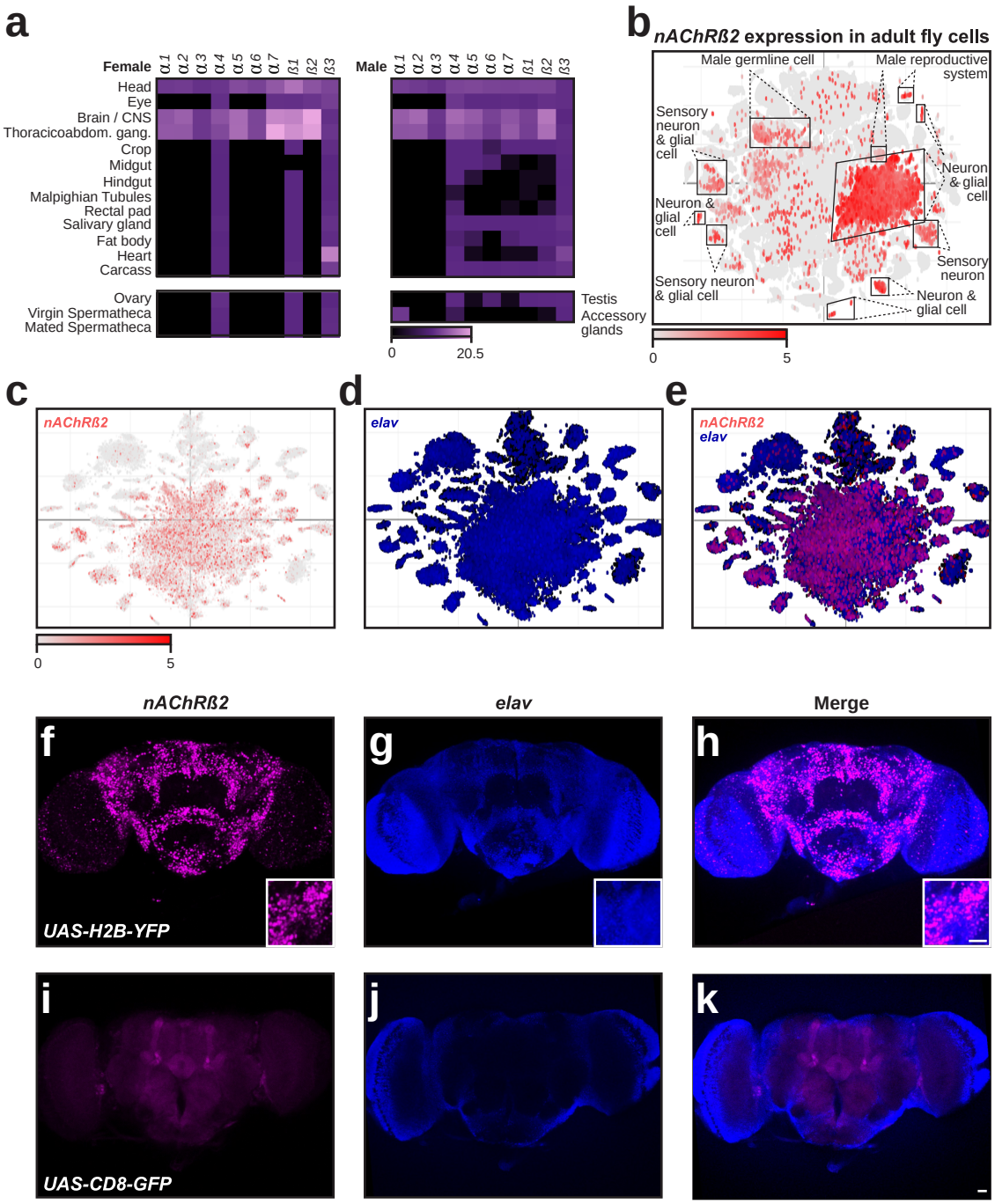
a
Female
α1 α2 α3 α4 α5 α6 α7 ß1 ß2 ß3
Head
Eye
Brain / CNS
Thoracicoabdom. gang.
Crop
Midgut
Hindgut
Malpighian Tubules
Rectal pad
Salivary gland
Fat body
Heart
Carcass
Ovary
Virgin Spermatheca
Mated Spermatheca
Male
Testis
Accessory glands
0
20.5
b
nAChRß2 expression in adult fly cells
Male germline cell
Male reproductive system
Sensory neuron & glial cell
Neuron & glial cell
Neuron & glial cell
Sensory neuron
Sensory neuron & glial cell
Neuron & glial cell
0
5
c
nAChRß2
0
5
d
elav
e
nAChRß2
elav
nAChRß2
elav
Merge
f
UAS-H2B-YFP
g
h
i
UAS-CD8-GFP
j
k

Figure 3

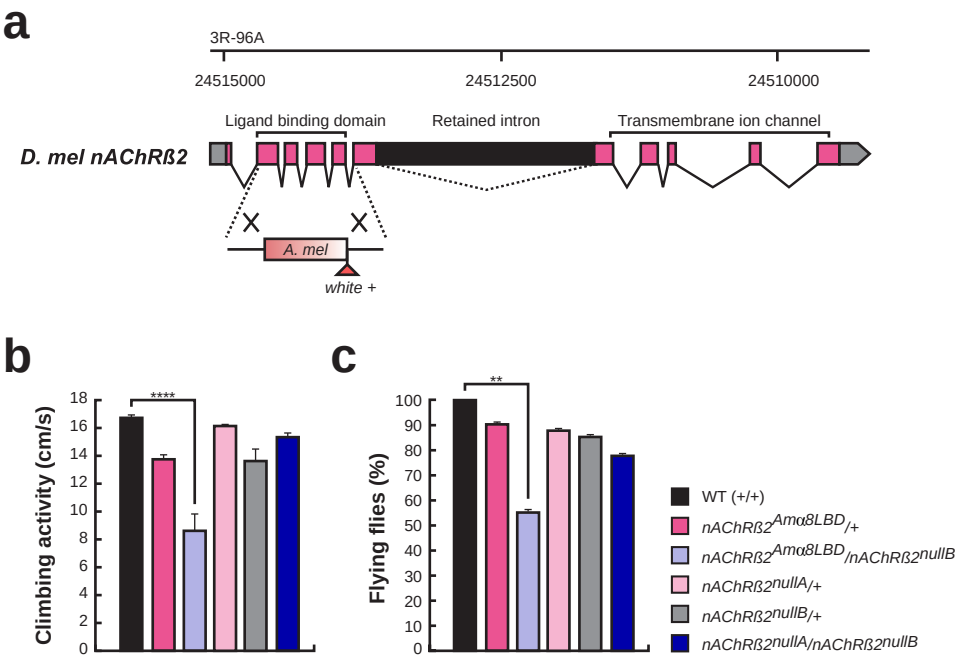
a
3R-96A
24515000
24512500
24510000
Ligand binding domain
Retained intron
Transmembrane ion channel
D. mel nAChRß2
A. mel
white +
b
Climbing activity (cm/s)
****
c
Flying flies (%)
**
WT (+/+)
nAChRß2Amα8LBD/+
nAChRß2Amα8LBD/nAChRß2nullB
nAChRß2nullA/+
nAChRß2nullB/+
nAChRß2nullA/nAChRß2nullB

Figure 4

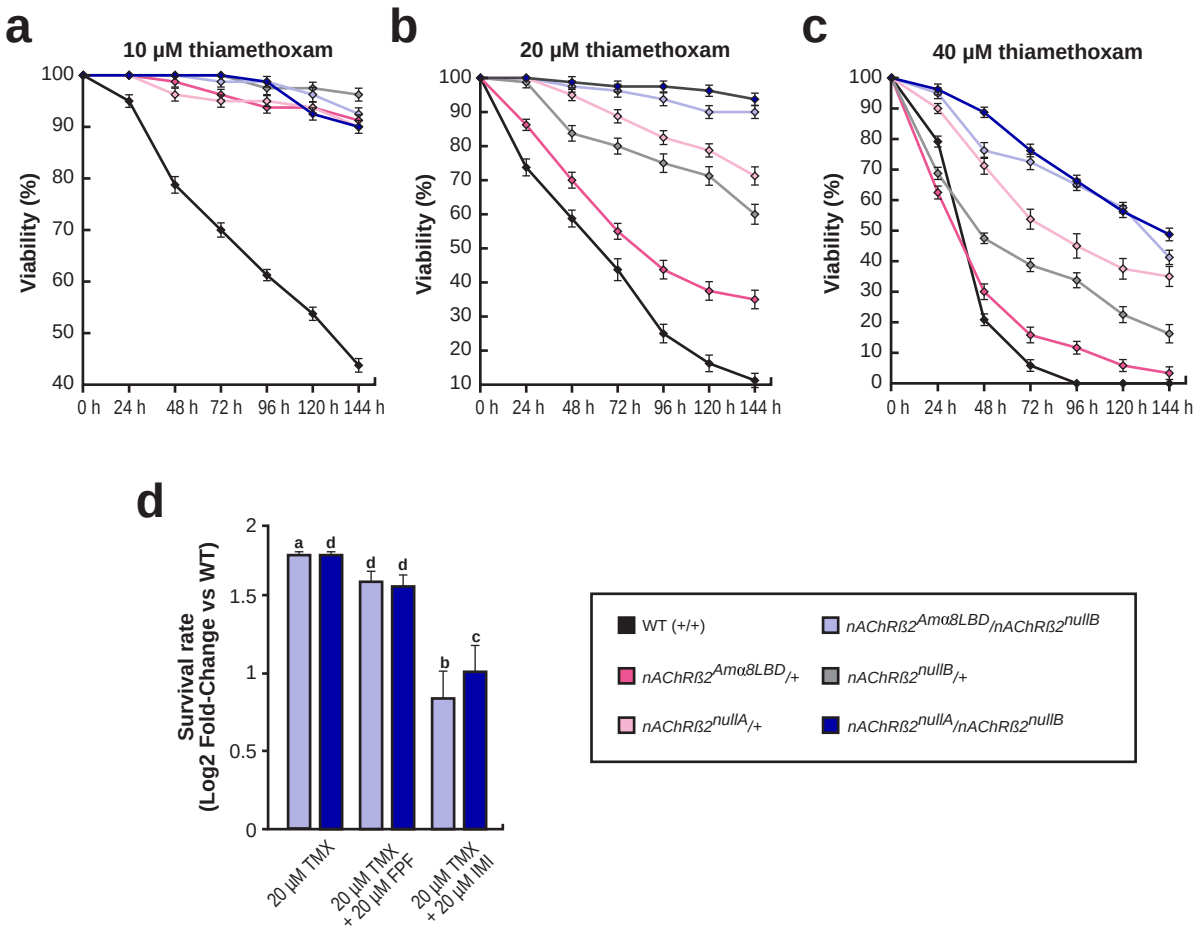
a
10 µM thiamethoxam
Viability (%)
100
90
80
70
60
50
40
0 h
24 h
48 h
72 h
96 h
120 h
144 h
b
20 µM thiamethoxam
Viability (%)
100
90
80
70
60
50
40
30
20
10
0 h
24 h
48 h
72 h
96 h
120 h
144 h
c
40 µM thiamethoxam
Viability (%)
100
90
80
70
60
50
40
30
20
10
0
0 h
24 h
48 h
72 h
96 h
120 h
144 h
d
Survival rate
(Log2 Fold-Change vs WT)
2
1.5
1
0.5
0
a
d
d
d
b
c
20 µM TMX
20 µM TMX
+ 20 µM FPF
20 µM TMX
+ 20 µM IMI
WT (+/+)
nAChRß2Amα8LBD/nAChRß2nullB
nAChRß2Amα8LBD/+
nAChRß2nullB/+
nAChRß2nullA/+
nAChRß2nullA/nAChRß2nullB